



## Short communication

## A triazole-based polymer electrolyte membrane for fuel cells operated in a wide temperature range (25–150 °C) with little humidification

Min-Kyu Song<sup>1</sup>, Xiaobing Zhu<sup>1</sup>, Meilin Liu\*

School of Materials Science and Engineering, Georgia Institute of Technology, Atlanta, GA 30332-0245, USA

## HIGHLIGHTS

- 1H-1,2,4-triazole grafted polysiloxane greatly enhances proton transport in PEM.
- Triazole-based PEM has high conductivity in low humidity at 25–100 °C.
- Fuel cells based on the new PEM demonstrated promising performance.
- The triazole-based new PEM may dramatically simplify fuel-cell systems.

## ARTICLE INFO

## Article history:

Received 15 November 2012

Received in revised form

8 March 2013

Accepted 5 April 2013

Available online 23 April 2013

## Keywords:

Fuel cells

Triazole

Polymer membrane

Low humidity

High temperature

## ABSTRACT

The development of polymer electrolyte membrane (PEM) fuel cells that can be operated over a wide temperature range without the need for humidification is highly desirable for vehicle applications to overcome the problems associated with CO poisoning and water management. Here we report a novel PEM based on 1H-1,2,4-triazole grafted polysiloxane doped with phosphoric acid and reinforced with porous expanded-polytetrafluoroethylene (ePTFE) film. Both bulk resistances and interfacial polarization resistances of the fuel cells based on this membrane were determined using impedance spectroscopy. Results indicate that the proton conductivities of the PEM have little dependence on operation temperature while the PEM fuel cells demonstrated good performance under very low humidity in a wide temperature range (from room temperature to more than 100 °C). The triazole-based new PEM may dramatically simplify the fuel-cell systems, offering great potential for mobile applications.

© 2013 Elsevier B.V. All rights reserved.

## 1. Introduction

Polymer electrolyte membrane (PEM) fuel cells are considered the next generation of power sources for zero emission vehicles due to high energy conversion efficiency and minimal pollutants [1]. Although PEM fuel cells have tremendous potential to replace automobile internal combustion engines, many challenges still remain [2]. Most of these challenges are associated with an intrinsic property of conventional polymer electrolyte membranes, the need for water as a proton carrier.

The most widely-used electrolytes for PEM fuel cells are perfluorinated sulfonic acid (PFSA)-type polymer membranes, such as Nafion, which shows adequate proton conductivity only in hydrated form [3]. The hydration requirement of a PFSA membrane

limits the maximum operation temperature of fuel cells to below the boiling point of water, i.e., 100 °C under atmospheric pressure. The limited operation temperature (typically 60–80 °C) requires very expensive platinum catalysts to increase the kinetics of the electrode reactions. Additionally, only high purity hydrogen gas can be used for the anode because even trace amounts of CO can easily poison platinum catalysts [4]. The hydrated membrane can suffer from degradation due to freeze/thaw cycling in outdoor applications (e.g. fuel-cell vehicles in a winter season) [5]. The humidification requirement of PFSA type membranes also raises another critical issue, the difficulty of implementing water-management strategies [6]. Thus, a voluminous humidifier and water-management systems are necessary to maintain stable performance in this type of fuel cells.

In this regard, fuel-cell operation above 100 °C under low-humidity conditions is highly desirable because it can enhance the rate of the electrochemical reactions on both the anode and cathode, improve the CO tolerance, and eliminate or simplify a cumbersome water-management system [7,8]. For automotive

\* Corresponding author. Tel.: +1 404 894 6114; fax: +1 404 894 9140.

E-mail address: [meilin.liu@mse.gatech.edu](mailto:meilin.liu@mse.gatech.edu) (M. Liu).<sup>1</sup> These authors contributed equally to this work.

applications, high-temperature operation without external humidification can reduce the size of the cooling system (i.e., radiator) and humidifier, thus increasing specific power density ( $\text{kW L}^{-1}$  or  $\text{kW kg}^{-1}$ ) of the overall fuel-cell system. Therefore, the development of a novel proton PEM that can operate at high temperature ( $>100\text{ }^\circ\text{C}$ ) under an anhydrous condition is vital to the commercialization of fuel-cell vehicles.

To date, various approaches have been explored to develop novel electrolytes operable at temperatures above  $100\text{ }^\circ\text{C}$ , including modified Nafion [9–11], alternative sulfonated polymers [12], and heterocycle and acid based polymers [7,13]. Among them, the PEMs based on phosphoric acid-doped polybenzimidazole (PBI) have gained the most attention because of the high proton conductivity in an anhydrous form and good thermal stability [14,15]. However, a PBI-based membrane shows very low proton conductivity at room temperature [7], requiring a long start-up time, which is not desirable for fuel-cell vehicle applications. Therefore, the development of new anhydrous proton conducting materials, functional under low-humidity conditions in a wide temperature range (from room temperature to above  $100\text{ }^\circ\text{C}$ ) with high proton conductivity and good stability, is vital to the commercialization of fuel-cell vehicles.

Our group first demonstrated triazole as an effective protogenic group to replace water and imidazole as proton carrier in PEMs for high-temperature operation [16–18]. Additional studies suggest that these PEMs have high proton conductivity in an anhydrous state and good electrochemical stability under fuel-cell operation conditions [19–25]. Here we report a novel PEM consisting of 1*H*-1,2,4-triazole grafted polysiloxane, doped with phosphoric acid and reinforced with expanded-polytetrafluoroethylene (ePTFE) film, prepared using a modified sol–gel process. Due to the unique molecular structure and membrane microstructure, this novel membrane exhibited both high proton conductivity under very low-humidity conditions and good thermal stability. PEM fuel-cells employing triazole-based novel membranes showed very little dependence of proton conductivity on operation temperature, demonstrating excellent performance not only at high temperatures (above  $100\text{ }^\circ\text{C}$ ) but also at room temperature under ambient pressure.

## 2. Experimental

We synthesized triazole-bearing polymers by grafting 1*H*-1,2,4-triazole to a polysiloxane backbone through nucleophilic substitution ( $\sim 50.4\text{ wt.}\%$  1,2,4-triazole in grafted polysiloxane triazole), then fabricated novel polymer membranes using an in-situ polymerization (sol–gel) process under the presence of phosphoric acid as the catalyst and the dopant with the reinforcement of porous ePTFE film. 1,2,4-triazole grafted polysiloxane (prepared as described elsewhere [18]) was mixed with tetraethyl orthosilicate (TEOS) and bis(ethanoxysilane)octane (Si-C<sub>8</sub>) organosiloxane (as cross-linkers) at a mass ratio of 2:1:1 (total 0.5 g) in a mixture (5 ml) of methanol and ethanol (1:1 v/v) under stirring for 24 h to allow for sufficient hydrolysis and condensation of the sol solution. A separate solution containing 0.4 g of phosphoric acid (85%) in a mixture (7 ml) of methanol and ethanol (1:1 v/v) was added into the sol solution prepared beforehand and the mixture was stirred for additional 15 min. Phosphoric acid was used as both the catalyst to complete the sol–gel reaction and the acidic dopant. Then each 4 ml of the resulting mixture was casted into three expanded ePTFE films (Donaldson) supported on plastic moulds with a diameter of 40 mm. During the gelation/drying process at room temperature, the solvents evaporation rate should be controlled carefully, to avoid precipitation of white particles. After drying for 3–4 days, the membrane was hot-pressed at  $200\text{ }^\circ\text{C}$  and 0.6 GPa.

The membranes were then immersed in concentrated phosphoric acid solution for 1 day (for doping of free acid). The phosphoric acid-doped triazole membranes were taken out, wiped-out and dried inside the oven at  $120\text{ }^\circ\text{C}$ . The typical thickness of membrane was  $\sim 50\text{ }\mu\text{m}$ . We measured the weight increase after the as-prepared membranes were immersed in free acid for 24 h, followed by drying at  $120\text{ }^\circ\text{C}$  for 24 h. The average weight gain was about 13 wt.%, implying that additional 13 wt.% of PA was doped into the membranes. If the PA-doping level is defined as the molar ratio of the PA per triazole ring [26], the PA-doping level of triazole-based membranes was estimated to be  $\sim 1.9\text{ mol}$  and  $\sim 2.15\text{ mol}$  of PA per mole of triazole ring before and after immersion in free acid. The PA-doping level of triazole-based membrane is still lower than those of the PBI-based membranes (e.g., 6–32 mol PA per PBI repeat unit) as reported in the literature [26–28]. The gas diffusion electrodes (GDEs) were fabricated by mixing a suitable amount of 1,2,4-triazole grafted polysiloxane with commercial 40% Pt/C catalysts (1,2,4-triazole grafted polysiloxane: Pt/C = 1:10 w/w) in the presence of phosphoric acid (0.5 g for  $25\text{ cm}^2$ ) in an ethanol/methanol mixture (1:1 v/v), and casting this catalyst ink onto a commercial gas diffusion layer (GDL, E-Tek). The loading amount of Pt was controlled at  $1\text{ mg cm}^{-2}$ . For the evaluation of fuel-cell performances, dry and wet  $\text{H}_2$  and  $\text{O}_2$  gas were used (the wet refers to humidification by bubbling the gas through a water bubbler kept at room temperature). The wet gas has a 3 v% water vapour, corresponding to 100% relative humidity at  $25\text{ }^\circ\text{C}$ . Thus, the relative humidity (RH, %) of the wet gas at  $150\text{ }^\circ\text{C}$ ,  $120\text{ }^\circ\text{C}$ ,  $105\text{ }^\circ\text{C}$ ,  $95\text{ }^\circ\text{C}$ ,  $80\text{ }^\circ\text{C}$ , and  $50\text{ }^\circ\text{C}$  was estimated to be 0.6%, 1.6%, 2.6%, 3.7%, 6.7%, and 26%, respectively.

Proton conductivities of triazole-based membranes and the interfacial polarization resistance of triazole-based electrodes were measured in dry  $\text{H}_2$  and  $\text{O}_2$  using impedance spectroscopy (Solartron 1286 and 1255) under the influence of an ac voltage of 10 mV in the frequency range of 0.01 Hz–1 MHz.

## 3. Results and discussion

1*H*-1,2,4-triazole has a molecular structure similar to that of imidazole, as schematically shown in Fig. 1, but its pK<sub>a</sub> values are much lower than those of imidazole [29], implying that 1*H*-1,2,4-triazole may have lower electron density. We synthesized a membrane that consists of 1*H*-1,2,4-triazole grafted polysiloxane, doped with phosphoric acid using a modified sol–gel process, and reinforced with ePTFE to improve the mechanical property. To evaluate the performance of this membrane in a fuel cell under practical operating conditions, we combined a  $50\text{ }\mu\text{m}$  thick triazole-based PEM with two GDEs to form a membrane-electrode-assembly (MEA). The membrane-electrode-assembly (MEA) was fabricated by pressing the two GDEs onto the PEM at  $120\text{ }^\circ\text{C}$  under a pressure of  $250\text{ kg cm}^{-2}$ . For Nafion212 membranes (Dupont), commercial GDEs (E-Tek,  $1\text{ mg cm}^{-2}$  Pt, PTFE binder) were used to prepare hot-pressed MEAs under the same conditions.

The open circuit voltage (OCV) of the cell was monitored at different temperatures in dry gas under ambient pressure. As shown in Fig. 2, the OCVs of the cells were sufficiently high (above 0.95 V) over a wide temperature range, implying that the PEM prepared by a modified sol–gel process is sufficiently dense even at high temperatures above  $100\text{ }^\circ\text{C}$  under dry conditions without significant gas crossover. This is quite promising because a commercially available Nafion212 membrane has small pores under dry conditions; reactant gases ( $\text{H}_2$  and  $\text{O}_2$ ) can directly mix through the membrane and this can be a cause of OCV drop as shown in Fig. 2, which may also lead to membrane degradation, lowering the efficiency and lifetime of fuel cells [30]. The OCV of PA-

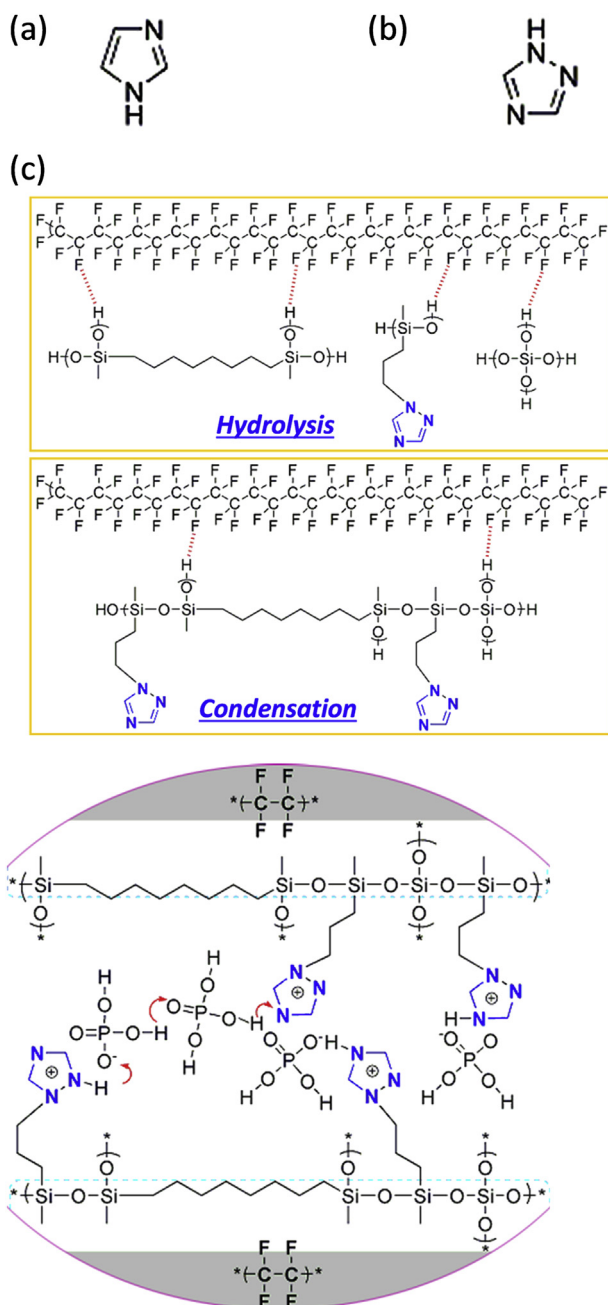


**Fig. 1.** Molecule structures of (a) imidazole, (b) 1H-1,2,4-triazole, and (c) schematic of fabrication procedure and proposed proton conduction mechanism of novel membranes containing 1,2,4-triazole grafted polysiloxane cross-linked with Si-C<sub>8</sub> and TEOS, doped with phosphoric acid and reinforced with ePTFE.

doped PBI system is typically around 0.9 V or higher at 160 °C under dry conditions [26].

Fig. 3 shows some typical current–voltage relationships and power density curves for triazole-based fuel cells operated at different temperatures (25, 50, 80, 95, 105, 120 and 150 °C) with dry H<sub>2</sub> and O<sub>2</sub> under ambient pressure. It should be noted that, for this performance study, the flow rates of the reactant gases (H<sub>2</sub> and O<sub>2</sub>) were kept at 50 mL min<sup>-1</sup> to both the anode and the cathode in order to minimize the effect of a gas transport limitation on performance. Clearly, the performance of triazole-based fuel cells increased with increasing temperature under dry conditions. The short-circuiting current density increased from 1070 mA cm<sup>-2</sup> at 25 °C to 1350 mA cm<sup>-2</sup> at 150 °C, and the peak power density

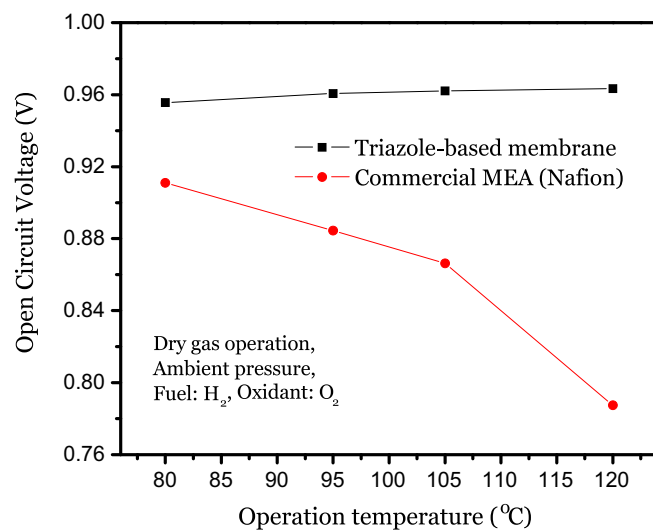


**Fig. 2.** Open circuit voltage of triazole-based and commercial Nafion212-based fuel cells monitored at different temperatures (80–120 °C) in low-humidity gas (H<sub>2</sub> and O<sub>2</sub>) environment.

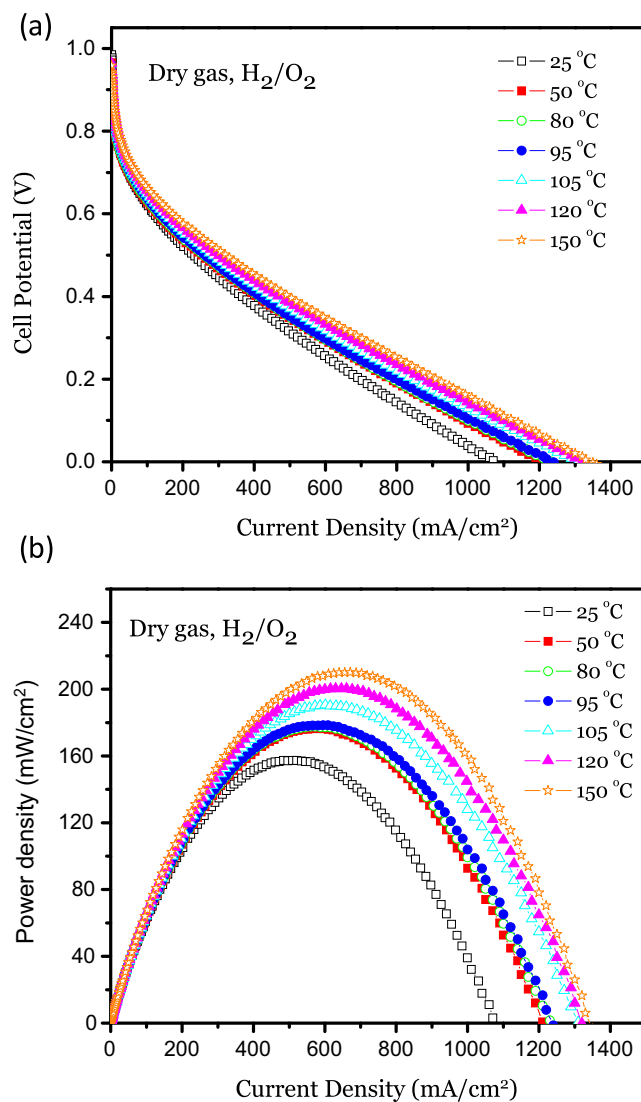


**Fig. 3.** (a) Cell voltages and (b) power densities as a function of current density for triazole-based fuel cells operated at different temperatures under low-humidity conditions.

increased from  $157 \text{ mW cm}^{-2}$  at  $25^\circ\text{C}$  to  $210 \text{ mW cm}^{-2}$  at  $150^\circ\text{C}$ . The performance demonstrated here (e.g.  $\sim 200 \text{ mA cm}^{-2}$  at  $0.6 \text{ V}$  at  $150^\circ\text{C}$ ,  $0.6\% \text{ RH}$ ) is lower than that (e.g.  $\sim 1000 \text{ mA cm}^{-2}$  at  $0.6 \text{ V}$  at  $65^\circ\text{C}$ ,  $100\% \text{ RH}$ ) of a commercial Nafion-based membrane (from Dupont) when fully humidified [31]. However, the performance of Nafion-based fuel cells decreases dramatically with increasing temperature because Nafion is not functional at high temperature under dry conditions [32]. Many attempts have been made to overcome drawbacks from the dry operation by increasing operation pressure up to 3–5 atm with a pressurized system [33–35] to eliminate a voluminous humidifier, which however, is also spacious and unfavourable for automotive applications.

It is noted that the performance of the triazole-based membrane with a PA-doping level of  $\sim 2.15 \text{ mol PA}$  per triazole ring is lower than those of the PBI-based membranes with PA-doping levels of 6–32 mol PA per PBI repeat unit [26–28]. For example, the highest power output ( $\sim 900 \text{ mW cm}^{-2}$  at  $160^\circ\text{C}$ ) was reported for the membranes with 32 mol PA per PBI repeat unit [26]. A fuel cell based on a commercial PBI-type membrane (from PEMEAS Fuel Cell Technologies) also showed improved high performance at high temperature (e.g. the peak power density increased from  $\sim 360 \text{ mW cm}^{-2}$  at  $120^\circ\text{C}$  to  $\sim 540 \text{ mW cm}^{-2}$  at  $200^\circ\text{C}$ ) [36], however, the performance drops rapidly as the operating temperature is reduced, due primarily to lower proton conductivity of the PBI-based membrane at lower temperatures [7]. It also has a long start-up time, making it necessary to have an auxiliary power unit. In contrast, the triazole-based fuel cells operated under an ambient

pressure with dry gas showed good performance over a wide temperature range, from room temperature to more than  $100^\circ\text{C}$ .

To more closely examine the effect of operating temperature on performance, a set of impedance spectra were collected at a constant cell voltage (i.e., DC polarization vs. OCV) to distinguish the individual performance loss caused by membrane resistance and the interfacial polarization resistance of the electrodes. Fig. 4 shows some typical Nyquist plots of impedance spectra collected at different temperatures under different DC polarization conditions. The insert in Fig. 4(a) shows an equivalent circuit used to interpret the impedance data. The first intercept in the high frequency region on the real axis represents the ohmic resistance (dominated by the membrane resistance) for proton conduction under a real fuel-cell operating condition. The diameter of the semicircle represents the interfacial polarization resistance of the two electrodes, a combination of the resistance to charge transfer associated with the electrochemical reactions taking place on two electrodes and the resistance to mass transfer of electro-active species to or away from the active sites. It was observed that the interfacial polarization resistance of electrodes decreased dramatically with the operation temperature, while ohmic resistance of the membrane was relatively independent of temperature. The performance losses due to gas transport may be relatively small in these experiments because the reactant gases were supplied to both electrodes at a relatively high flow rate.

The measured ohmic resistance and the electrode polarization resistance are plotted as a function of operation temperature. Fig. 5

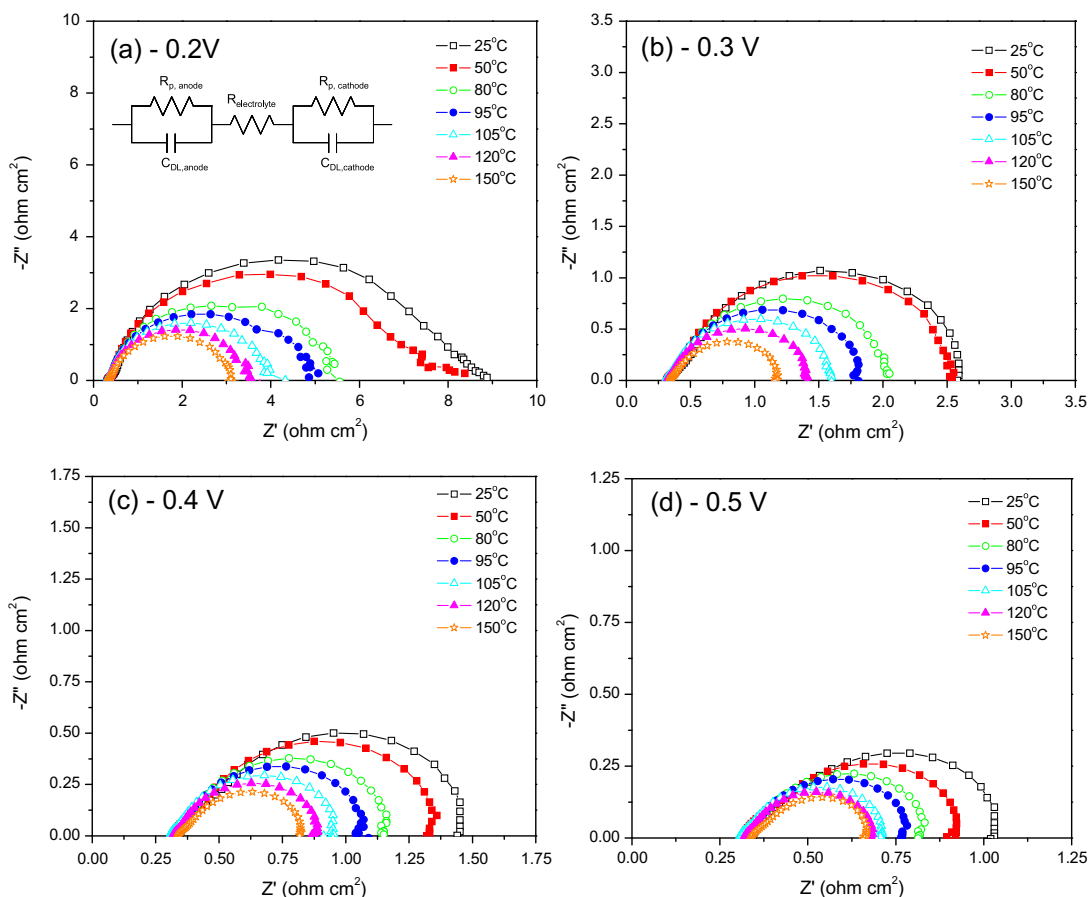
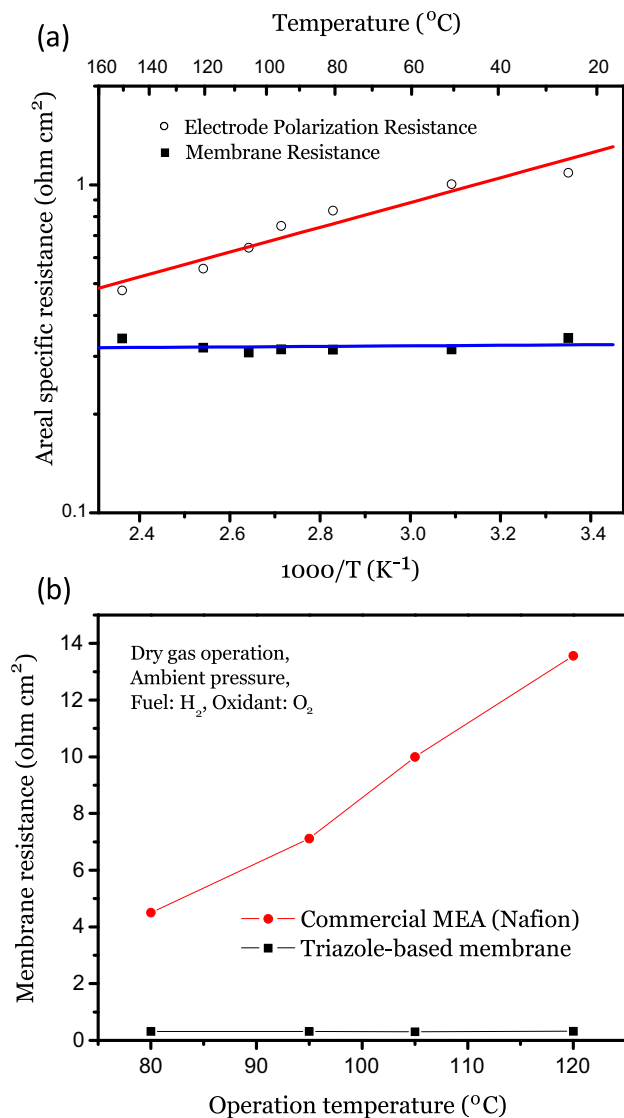
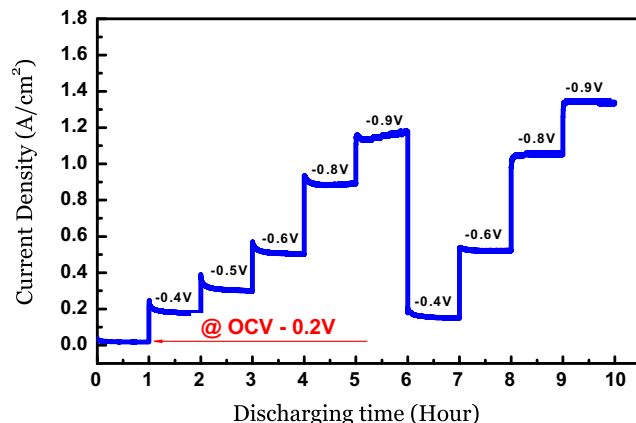


Fig. 4. Typical impedance spectra (Nyquist plot) collected with dry  $\text{H}_2/\text{O}_2$  at ambient pressure under various DC polarizations: (a)  $-0.2 \text{ V}$  vs. OCV; (b)  $-0.3 \text{ V}$  vs. OCV; (c)  $-0.4 \text{ V}$  vs. OCV; (d)  $-0.5 \text{ V}$  vs. OCV.



**Fig. 5.** (a) Temperature dependence of electrode polarization resistance (estimated from DC polarization of  $-0.4$  V vs. OCV) and membrane resistance of triazole-based fuel cells operated at different temperatures under low-humidity conditions. Membrane resistance was averaged. (b) Comparison of ohmic resistance of Nafion-based and triazole-based fuel cells run on dry H<sub>2</sub> and O<sub>2</sub> at different temperatures.

shows that ohmic resistance of the membrane was relatively independent of temperature (from  $0.342 \Omega \text{ cm}^2$  at  $25^\circ\text{C}$  to  $0.34 \Omega \text{ cm}^2$  at  $150^\circ\text{C}$  under DC polarization of  $-0.4$  V vs. OCV), implying that novel membranes have good proton conductivity under dry conditions, and have little dependence on temperature. The observed small dependence of proton conductivity on temperature under low-humidity conditions is very encouraging, especially for an automotive application which requires that the electrolyte membrane be functional in dry gas at high temperatures. The anhydrous proton conducting mechanism of a triazole-based membrane is not yet clearly understood, and requires further extensive study to elucidate the proton conduction mechanism. The measured membrane resistance is a little bit higher than those ( $0.08$ – $0.11 \Omega \text{ cm}^2$ ) of the commercial PBI-based membranes at high temperatures ( $160$  and  $200^\circ\text{C}$ ) [36], but the performance loss from ohmic resistance of the membranes is expected to be reduced by decreasing the electrolyte thickness below  $20 \mu\text{m}$ . This is possible



**Fig. 6.** Cyclic performance of triazole-based fuel cells operated at  $120^\circ\text{C}$  in a dry gas (H<sub>2</sub> and O<sub>2</sub>) environment at ambient pressure under different DC polarizations.

because the membranes reinforced by ePTFE showed good mechanical properties and low gas permeability.

The interfacial polarization resistance of triazole-based electrodes appeared to be higher at lower overpotentials (DC polarization vs. OCV, e.g. Fig. 4(a)), indicating that the charge-transfer resistance of the electrode (i.e., activation polarization) is likely the major cause of the performance loss in triazole-based PEM fuel cells over a wide temperature range. As expected, however, electrode polarization resistances decreased dramatically with an increase in operation temperature (from  $1.43 \Omega \text{ cm}^2$  at  $25^\circ\text{C}$  to  $0.48 \Omega \text{ cm}^2$  at  $150^\circ\text{C}$  under DC polarization of  $-0.4$  V vs. OCV) because the electrochemical reactions on the electrodes are thermally-activated processes. This result clearly shows the advantage of high-temperature operation above  $100^\circ\text{C}$ . The charge-transfer resistance of PA-doped PBI system also decreased with an increase in operation temperature (from  $\sim 0.15 \Omega \text{ cm}^2$  at  $160^\circ\text{C}$  to  $\sim 0.13 \Omega \text{ cm}^2$  at  $200^\circ\text{C}$  under similar conditions) [36]. In contrast, for a Nafion-based fuel cell, performance diminishes with increasing operation temperature because of an increase in charge-transfer resistance [37]. This is attributed mostly to the decrease in proton conductivity of Nafion in membranes and in catalyst layers. An optimized microstructure for electrodes and improved fabrication techniques will be necessary to further reduce Pt loadings, and lower the electrode polarization resistance of triazole-based fuel cells.

Due to the anhydrous nature of the triazole-based membrane and electrodes, fuel-cell performances were very stable at high current density without flooding when operated at  $120^\circ\text{C}$  with dry O<sub>2</sub> and H<sub>2</sub> gas under ambient pressure, as shown in Fig. 6. It implies that triazole-based fuel cells can potentially eliminate the voluminous water-management system. Further study will be performed to extend the operation temperature of triazole-based fuel cells down to  $-20^\circ\text{C}$  and up to  $200^\circ\text{C}$ . The peak power densities of triazole-based fuel cells are shown in Fig. 7 as a function of operation temperature (from  $157 \text{ mW cm}^{-2}$  at  $25^\circ\text{C}$  to  $210 \text{ mW cm}^{-2}$  at  $150^\circ\text{C}$ ). Although the performance demonstrated here is lower than those of the PBI-type membranes (from  $\sim 360 \text{ mW cm}^{-2}$  at  $120^\circ\text{C}$  to  $\sim 540 \text{ mW cm}^{-2}$  at  $200^\circ\text{C}$ ) [36], a fundamental understanding of the anhydrous proton conduction mechanism may lead to rational design of better PEMs for fuel-cell operation at a subzero temperature to mitigate degradation originated from freeze/thaw cycling. Additionally, the high boiling point ( $256^\circ\text{C}$ ) of 1,2,4-triazole and the good thermal stability of the membrane may allow the operation of fuel cells at temperatures up to  $200^\circ\text{C}$ .



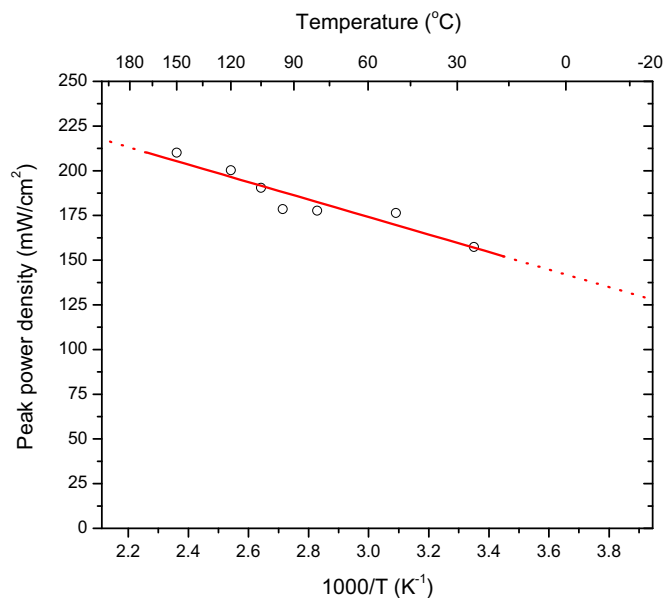


Fig. 7. The peak power density as a function of operating temperature for triazole-based fuel cells operated under low-humidity conditions at ambient pressure.

#### 4. Conclusions

In summary, fuel cells based on a triazole-type membrane demonstrated good performance in a wide temperature range (from room temperature to above 100 °C) in dry fuels and oxidant under ambient pressure. This novel membrane may allow a dramatic simplification of fuel-cell systems, which could facilitate the commercialization of fuel-cell vehicles. The fuel cells based on this membrane may also serve as power sources for other applications, where a wider range operation temperature is important without cumbersome humidification and pressurization systems such as military and space applications. Additional research will be necessary to improve the performance of triazole-based fuel cells further by decreasing membrane thickness (thus membrane resistance) and optimizing electrode composition and microstructure.

#### Acknowledgement

This material is based upon work supported as part of the Heterogeneous Functional Materials (HetroFoam) Center, an Energy Frontier Research Center funded by the U.S. Department of Energy, Office of Science, Office of Basic Energy Sciences under Award Number DE-SC0001061. It was also partially supported by Toyota Technology Center. The authors would like to gratefully acknowledge technical discussions with Dr. Zhen Zhou.

#### Appendix A. Supplementary data

Supplementary data related to this article can be found at <http://dx.doi.org/10.1016/j.jpowsour.2013.04.016>.

#### References

- [1] M. Winter, R.J. Brodd, *Chem. Rev.* 104 (2004) 4245–4270.
- [2] M. Schuster, T. Rager, A. Noda, K.D. Kreuer, J. Maier, *Fuel Cells* 5 (2005) 355–365.
- [3] M.A. Hickner, H. Ghassemi, Y.S. Kim, B.R. Einsla, J.E. McGrath, *Chem. Rev.* 104 (2004) 4587–4611.
- [4] Q. Li, R. He, J.O. Jensen, N.J. Bjerrum, *Chem. Mater.* 15 (2003) 4896–4915.
- [5] S. Kim, M.M. Mench, *J. Power Sources* 174 (2007) 206–220.
- [6] R.K. Ahluwalia, X. Wang, *J. Power Sources* 177 (2008) 167–176.
- [7] Q. Li, R. He, J.O. Jensen, N.J. Bjerrum, *Fuel Cells* 4 (2004) 147–159.
- [8] S.U. Celik, A. Bozkurt, S.S. Hosseini, *Prog. Polym. Sci.* 37 (2012) 1265–1291.
- [9] M. Doyle, S.K. Choi, G. Proulx, *J. Electrochem. Soc.* 147 (2000) 34–37.
- [10] K.T. Adjemian, S.J. Lee, S. Srinivasan, J. Benziger, A.B. Bocarsly, *J. Electrochem. Soc.* 149 (2002) A256–A261.
- [11] P. Dimitrova, K.A. Friedrich, U. Stimming, B. Vogt, *Solid State Ionics* 150 (2002) 115–122.
- [12] J.A. Kerres, *J. Membr. Sci.* 185 (2001) 3–27.
- [13] K.D. Kreuer, A. Fuchs, M. Ise, M. Spaeth, J. Maier, *Electrochim. Acta* 43 (1998) 1281–1288.
- [14] J.S. Wainright, J.T. Wang, D. Weng, R.F. Savinell, M. Litt, *J. Electrochem. Soc.* 142 (1995) L121–L123.
- [15] M.F.H. Schuster, W.H. Meyer, M. Schuster, K.D. Kreuer, *Chem. Mater.* 16 (2004) 329–337.
- [16] Z. Zhou, S. Li, Y. Zhang, M. Liu, W. Li, *J. Am. Chem. Soc.* 127 (2005) 10824–10825.
- [17] Z. Zhou, R. Liu, J. Wang, S. Li, M. Liu, J.-L. Brédas, *J. Phys. Chem. A* 110 (2006) 2322–2324.
- [18] S. Li, Z. Zhou, Y. Zhang, M. Liu, W. Li, *Chem. Mater.* 17 (2005) 5884–5886.
- [19] R. Subbaraman, H. Ghassemi, T.A. Zawodzinski, *J. Am. Chem. Soc.* 129 (2007) 2238–2239.
- [20] K. Je-Deok, T. Mori, S. Hayashi, I. Honma, *J. Electrochem. Soc.* 154 (2007) A290–A294.
- [21] S.U. Celik, U. Akbey, R. Graf, A. Bozkurt, H.W. Spiess, *Phys. Chem. Chem. Phys.* 10 (2008) 6058–6066.
- [22] R. Subbaraman, H. Ghassemi, T. Zawodzinski, *Solid State Ionics* 180 (2009) 1143–1150.
- [23] S. Sanghi, M. Tuominen, E.B. Coughlin, *Solid State Ionics* 181 (2010) 1183–1188.
- [24] Y. Sijia, Z. Songjun, S. Xiaolu, Y. Huijun, X. Yuanqin, X. Weijian, *Solid State Ionics Diffus. React.* 198 (2011) 1–55.
- [25] A. Li, T. Yan, P. Shen, *J. Power Sources* 196 (2011) 905–910.
- [26] L. Xiao, H. Zhang, E. Scanlon, L.S. Ramanathan, E.-W. Choe, D. Rogers, T. Apple, B.C. Benicewicz, *Chem. Mater.* 17 (2005) 5328–5333.
- [27] Y.-L. Ma, J.S. Wainright, M.H. Litt, R.F. Savinell, *J. Electrochem. Soc.* 151 (2004) A8–A16.
- [28] L. Qingfeng, H.A. Hjuler, N.J. Bjerrum, *J. Appl. Electrochem.* 31 (2001) 773–779.
- [29] R.A. Gagliano, R.C. Knowlton, L.D. Byers, *J. Org. Chem.* 54 (1989) 5247–5250.
- [30] W. Liu, D. Zuckerbrod, *J. Electrochem. Soc.* 152 (2005) A1165–A1170.
- [31] D.E. Curtin, R.D. Lousenberg, T.J. Henry, P.C. Tangeman, M.E. Tisack, *J. Power Sources* 131 (2004) 41–48.
- [32] J. Zhang, Y. Tang, C. Song, X. Cheng, J. Zhang, H. Wang, *Electrochim. Acta* 52 (2007) 5095–5101.
- [33] P. Staiti, A.S. Aricò, V. Baglio, F. Lufrano, E. Passalacqua, V. Antonucci, *Solid State Ionics* 145 (2001) 101–107.
- [34] P. Costamagna, C. Yang, A.B. Bocarsly, S. Srinivasan, *Electrochim. Acta* 47 (2002) 1023–1033.
- [35] C. Yang, S. Srinivasan, A.S. Arico, P. Creti, V. Baglio, V. Antonucci, *Electrochem. Solid State Lett.* 4 (2001) A31–A34.
- [36] J. Zhang, Y. Tang, C. Song, J. Zhang, *J. Power Sources* 172 (2007) 163–171.
- [37] Y. Tang, J. Zhang, C. Song, H. Liu, J. Zhang, H. Wang, S. Mackinnon, T. Peckham, J. Li, S. McDermaid, P. Kozak, *J. Electrochem. Soc.* 153 (2006) A2036–A2043.